

# OBSERVATIONS OF NEAR-INERTIAL INTERNAL WAVES AND MIXING IN THE SEASONAL THERMOCLINE

Charles C. Eriksen  
School of Oceanography WB-10  
University of Washington  
Seattle, WA 98195

## ABSTRACT

Wind forced near-inertial internal waves reduce gradient Richardson number sufficiently to induce microscale mixing within the seasonal pycnocline in eastern North Pacific observations. The net buoyancy change inferred from a moored time series of upper ocean observations implies turbulent dissipation rates sufficient to damp near-inertial kinetic energy in the mixed layer in several days.

## INTRODUCTION

Wind stress is well recognized as a source of both internal gravity waves and mixing in the upper ocean. Swiftly moving wind systems generate internal waves whose phase speeds match their translation speeds. Since most storms translate at speeds at the high end of the range of possible internal wave phase speeds, storm-generated internal waves tend to be only slightly superinertial in frequency (Kundu and Thomson, 1985; D'Asaro, 1989). While the details of how stress applied by the wind is transmitted through the upper ocean are far from clear, both observations and theoretical considerations point to nearly linear variation of stress through a surface mixed layer such that stress effectively vanishes only slightly deeper than this layer. Because there is a relatively sharp transition between acceleration in the mixed layer and the stratified region beneath it, strong shears are found at the base of the mixed layer. This shear, in turn, is responsible for continued deepening of a mixed layer, as recognized in model parameterizations (Pollard et al., 1973; Price et al., 1986). As this shear is dominated by variance at slightly superinertial frequencies, motions in the seasonal pycnocline take the form of propagating near-inertial internal gravity waves. Observations in the OCEAN STORMS program discussed here indicate that these wind-forced internal waves are sufficiently energetic to account for mixing implied by temporal evolution of upper ocean density structure.

## UPPER OCEAN CURRENT AND DENSITY STRUCTURE

The observations discussed here come from a single 10-month Profiling Current Meter (PCM) record collected at 47° 35' N, 139° 23' W in the eastern North Pacific. The record begins August 22, 1987 and ends June 12, 1988, spanning the complete fall and winter cooling periods and the beginning of spring warming. The PCM profiled every 4 hours, averaging currents, temperature, and electrical conductivity into 5 m thick bins from 195 to 35 m depth. The subsurface PCM mooring was set 15 m deeper than in other deployments in anticipation of the severe sea state expected (and encountered) in the OCEAN STORMS site. The upward profile transit routinely took 20 to 25 minutes to complete, as the instrument used an electric pump system to control its buoyancy, hence its movement along the upper section of the mooring. The unique feature of PCMs is that they collect simultaneous current and density profiles at fixed locations in the upper ocean over extended periods. The instruments are capable of collecting roughly 2000 profiles, depending on the depth to which profiles are made, the strength of ambient currents and water temperature. Details of the design and operation of the engineering prototype PCM are given in Eriksen et al. (1982).

Upper ocean density structure at the OCEAN STORMS site is dominated by two pycnoclines; the upper seasonal one is dominated by temperature stratification while the deeper permanent one is dominated by salinity stratification. During the course of the winter, the shallow seasonal pycnocline is not merely eroded by storm-induced mixing, it itself is deepened as the mixed layer deepens, as indicated in the density record contoured in Figure 1. From August through October, the PCM does not profile high enough in the water column to encounter the mixed layer. Over the course of November and December, the mixed layer both deepens and becomes more dense. The seasonal pycnocline maintains a thickness of about 20 m during this period whereafter it merges with the permanent pycnocline centered at roughly 115 m depth. Although the stratification remains weak at depths shallower than about 90 m from January through March, this part of the water column is not strictly uniformly well mixed. Restratification begins in April and by late May a new seasonal pycnocline is evident.

The current structure which accompanies these changes in stratification is dominated by near-inertial motions (inertial period  $2\pi/f=16.254$  hr) concentrated in the surface mixed layer but occasionally penetrating both the seasonal and permanent pycnoclines. The stick vector plot of currents in Figure 2 reveals an enormous burst of kinetic energy starting in early October at the shallowest depth profiled and appearing later deeper, suggestive of a wave packet propagating. High current largely is confined to the mixed layer as it deepens in November and December, but more bursts of high current in the pycnocline occur in January and less intensely through April and even May.

Near-inertial frequency motions dominate the spectrum of current for all depths and are particularly evident in the October storm event. An expanded view of density and current

# Mixing in the Seasonal Thermocline

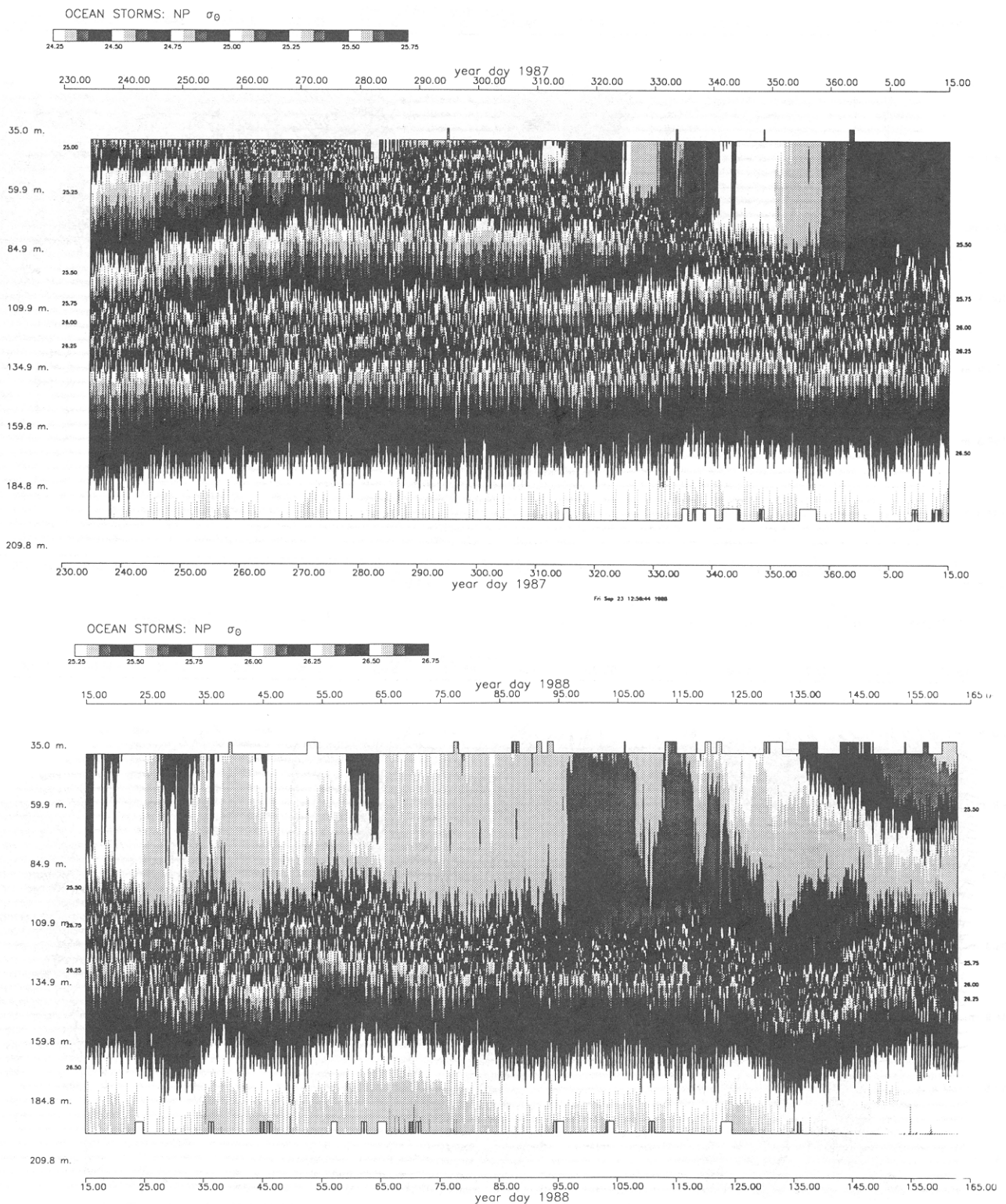


Figure 1. Potential density  $\sigma_{\theta 3}$  in 5-m depth bins every 4 hr contoured with a gray scale which repeats every 0.25 kg/m. The two frames start at 18 August 1987 (year day 230) and 15 January 1988 (year day 15), respectively, and depths are given at the left of each.

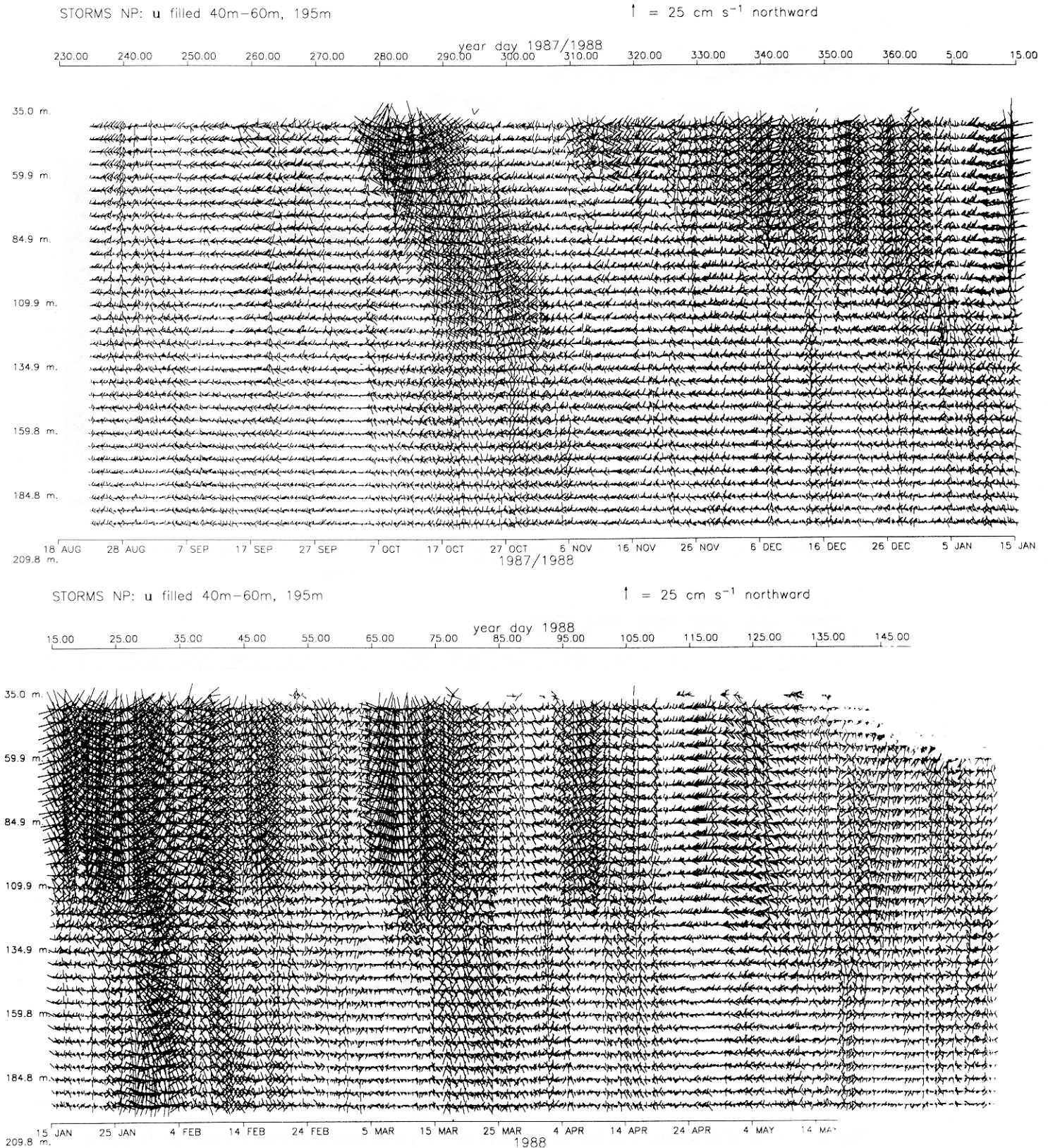


Figure 2. Current time series for each depth bin plotted as stick vectors where the scale is given at the upper right of each frame. The frames are the same as in Fig. 1.

is given in Figures 3 and 4 covering the period September 12 to November 1, 1987. Of particular interest is the jump in stratification structure which takes place on October 4 just beneath the seasonal pycnocline at depths from 55 to 75 m (Figure 3, left panel). This jump from weak to stronger stratification coincides with the appearance of strong near-inertial rotary currents (Figure 4, left panel). Density surfaces oscillate vertically with amplitudes as much as 10 m peak to peak with a near-inertial period in the week following the onset of the current burst. Interpreting these as due to vertical motion is consistent with regarding the horizontal currents as due to near-inertial internal waves with horizontal wavelengths of a few hundred km. A less prominent transition in density structure and near-inertial current activity can be found on September 14 at 40 to 50 m depth. Horizontal advection is inadequate to explain these density changes (as will be discussed below). The implication is that water within the pycnocline undergoes incomplete mixing in response to internal wave activity, that is, mixing which is sufficient to reduce but not eliminate stratification locally.

This mixing is accomplished through elevation of shear and accompanying reduction of Richardson number. Reduction of Richardson number is associated with shear instability, an idea confirmed by microstructure observations of turbulent mixing (Peters et al., 1988). Vertical shear increases to amplitudes as high as  $0.02 \text{ s}^{-1}$  in near-inertial waves in the October 4 storm (Figure 5). Elevated vertical shear is also apparent in the top three depth bins for which a 10 m centered first difference can be evaluated (45, 50, and 55 m) in the September 14 storm. Shear also tends to be somewhat higher within the permanent pycnocline, a feature presumed due to amplification of horizontal currents as internal waves propagate through a region of stronger stratification (e.g., WKB scaling). Gradient Richardson number  $Ri$  is the square of the ratio of buoyancy frequency  $N$  to vertical shear  $u_z$ , hence a plot of a vector whose components are  $N$  and  $u_z$  can reveal variations in both the stability of flow and the potential and kinetic energy associated with stratification and shear. Such a plot is given in Figure 6, where the slope of each stick vector relative to the time axis is the instantaneous inverse Richardson number  $Ri^{-1}$ . During both the October 4 and September 14 storms  $Ri$  reduces to unity or less.

### ESTIMATES OF MIXING RATES

The substantial changes in upper ocean stratification evident in this OCEAN STORMS PCM record strongly suggest that mixing is important in effecting these changes. Compared to other regions of the ocean, mesoscale eddy activity in the eastern North Pacific is relatively weak. Nevertheless, advection still makes significant contributions to density changes observed at a fixed location. In order to infer quantitative estimates of mixing activity from a sequence of profiles at a fixed location, estimates of horizontal and vertical advection of density must be added to the observed rate of density change so that their sum can be considered the convergence of microscale turbulent density flux. Consider the equations for density and horizontal momentum conservation:



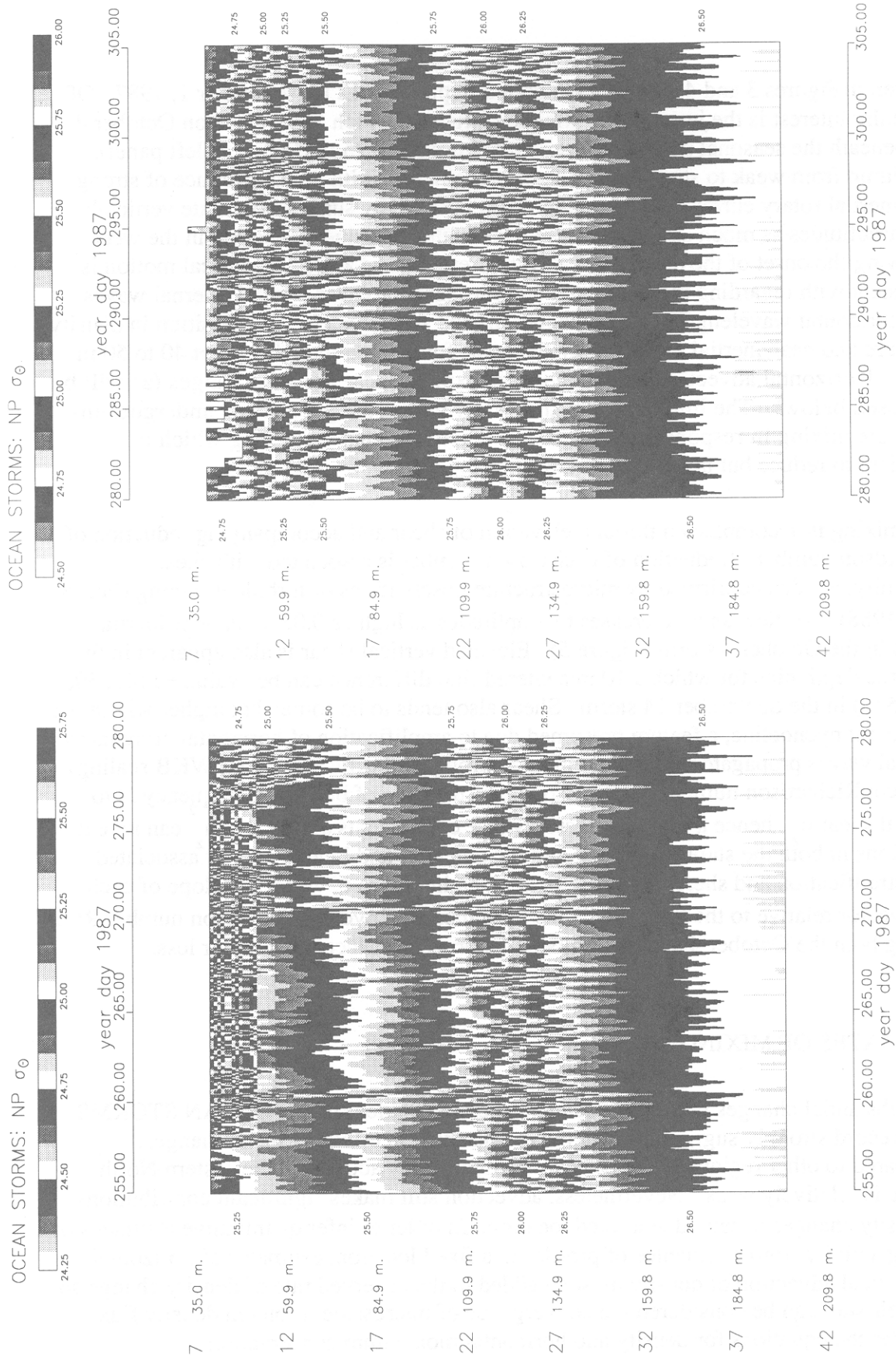


Figure 3. Expanded time scale contour plot of potential density  $\sigma_\theta$  for the period 12 September to 1 November 1987, otherwise as in Fig. 1. September 14 and October 4 are year days 257 and 277, respectively.

# Mixing in the Seasonal Thermocline

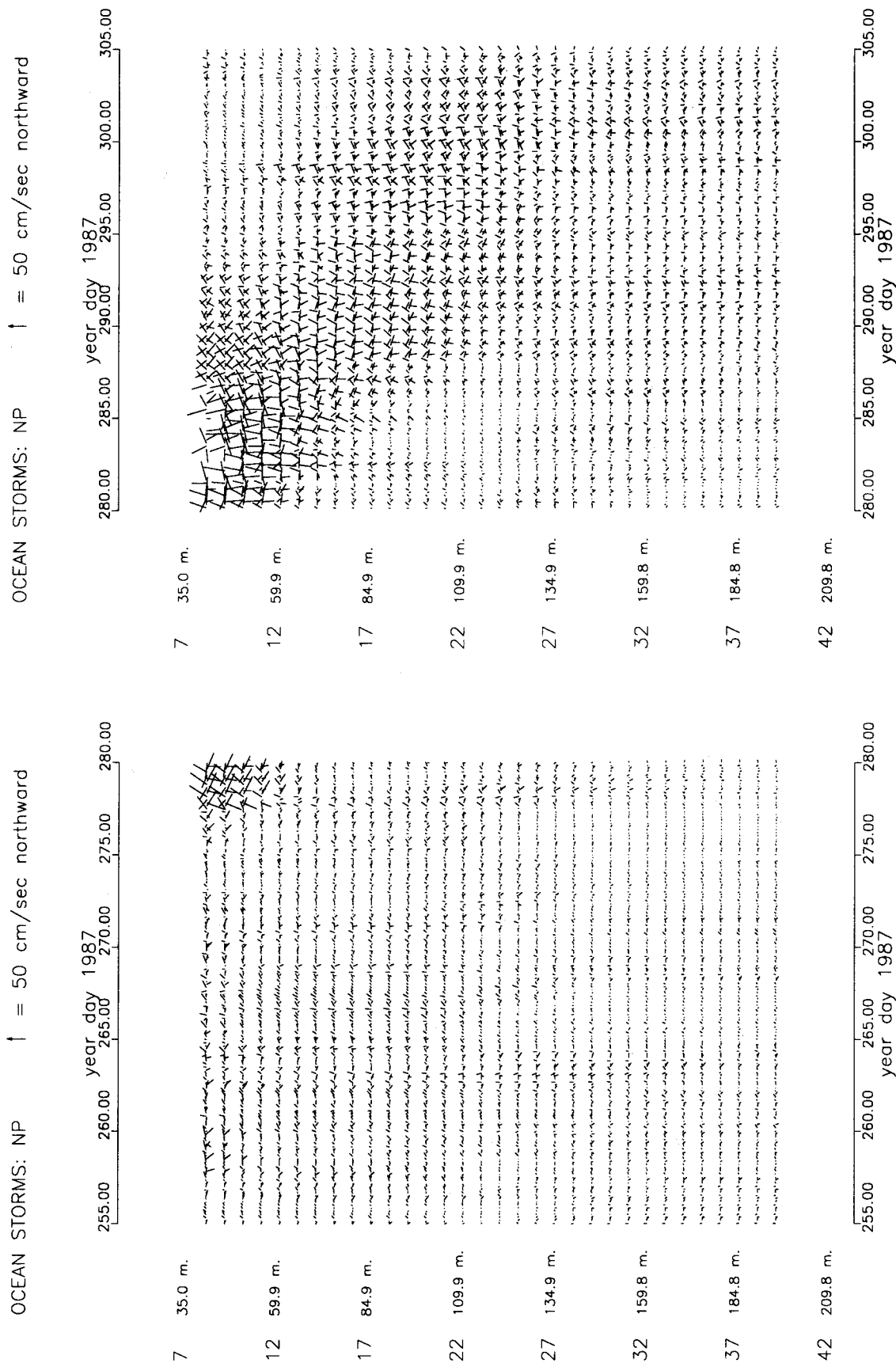


Figure 4. Expanded time scale current time series for the period shown in Fig. 3, otherwise as in Fig. 2.

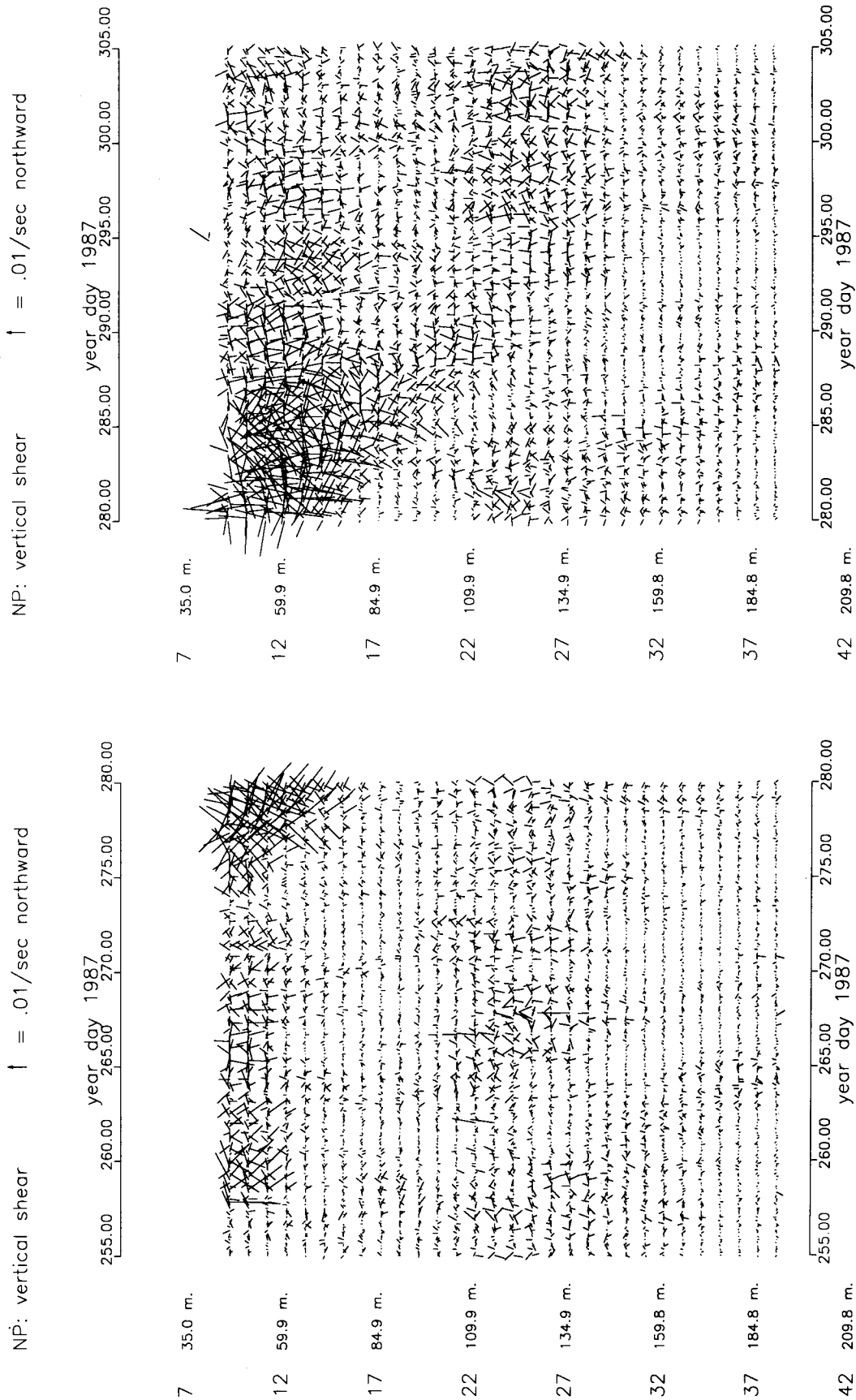


Figure 5. Vertical shear time series calculated as a center first difference over 10 m and plotted as stick vectors for the period shown in Fig. 3.



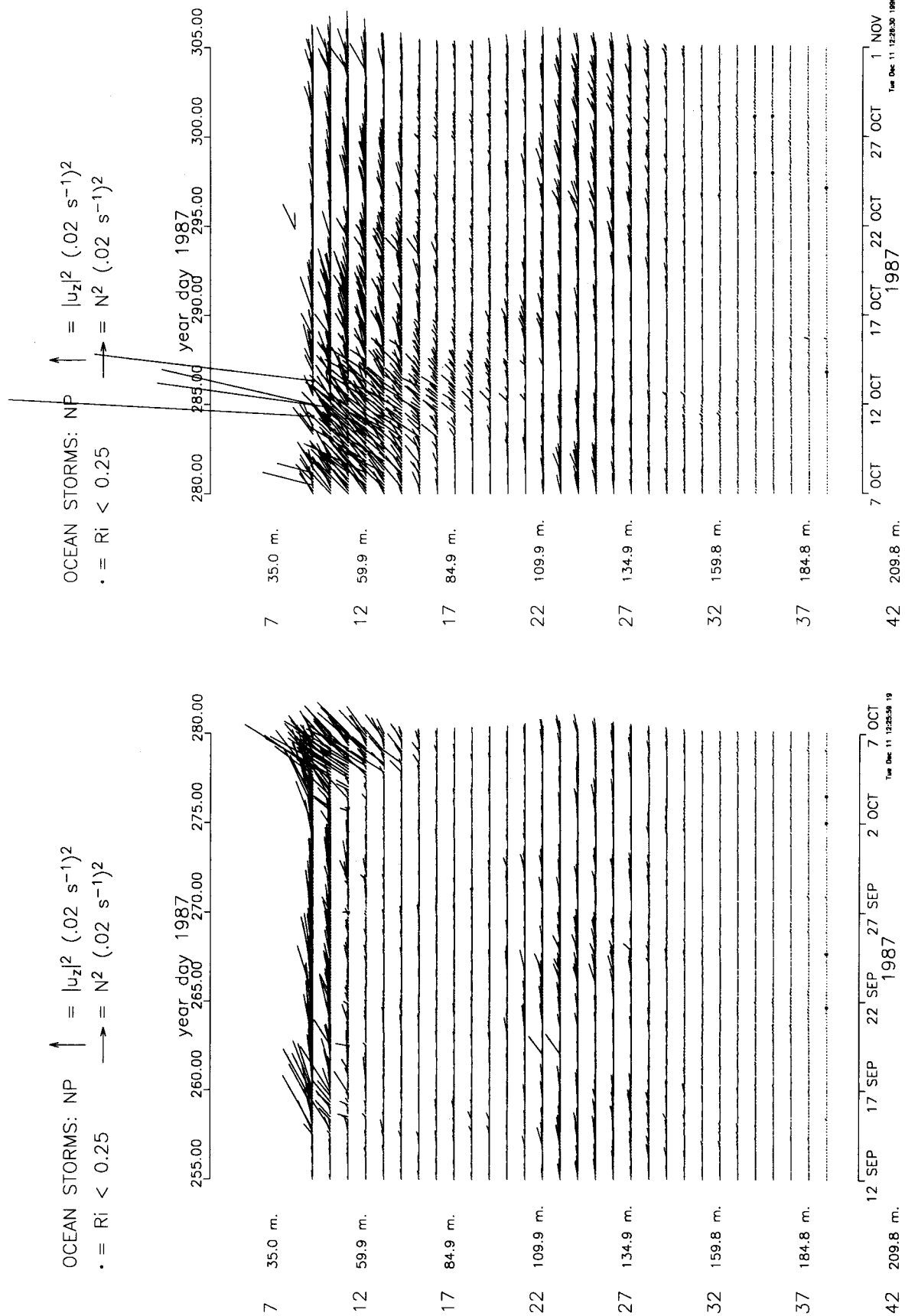


Figure 6. Vector time series of a quantity whose components are shear squared and buoyancy frequency squared plotted as in Figs. 4 and 5. The slope of each vector above the time axis is inverse Richardson number.

$$\rho_t + \mathbf{u} \cdot \nabla \rho + w \rho_z = -\langle w' \rho' \rangle_z \quad (1)$$

$$\mathbf{u}_t + \mathbf{u} \cdot \nabla \mathbf{u} + w \mathbf{u}_z + 2\Omega \times \mathbf{u} + \rho_0^{-1} \nabla p = -\langle \mathbf{u}' w' \rangle_z \quad (2)$$

where the primed quantities represent turbulent microscale variations and brackets the averages of their products. The first equation states that density changes following a particle are due solely to the vertical convergence of vertical turbulent transport of density. The second states that horizontal acceleration of a fluid parcel in a rotating frame of reference is balanced by a pressure gradient force and vertical convergence of vertical turbulent transport of horizontal momentum. Turbulence is considered as any process producing non-vanishing correlation between flow components at time and space scales too small to be resolved by the observations. It is also assumed that only vertical transports of density and momentum by turbulence are important. At low frequencies the momentum balance is geostrophic provided turbulent stresses  $\tau = -\rho_0 \langle \mathbf{u}' w' \rangle$  can be ignored. This simplification is poorest within the mixed layer and is of questionable validity within the seasonal pycnocline. Nevertheless, we make it here in order to obtain estimates of horizontal density gradients through the thermal wind equations. Then (1) may be written as

$$\rho_t - f \rho_0 g^{-1} (u v_z - v u_z) + w \rho_z = -\langle w' \rho' \rangle_z \quad (3)$$

where  $f = 2\Omega \sin(\text{latitude})$  is the inertial frequency. Since we are without direct measurements of vertical velocity, we must assume that turbulent mass fluxes  $\langle w' \rho' \rangle$  effectively vanish at some depth beneath the mixed layer so that  $w$  can be estimated from (3) for the restricted depth range for which density is assumed to change purely advectively. Since  $w$  must also effectively vanish at the sea surface because changes in sea level are very slight,  $w$  can be interpolated for the mixed layer and the depth range within the pycnocline for which mixing is presumed of potential importance. The linear inviscid modes of oscillation of a rotating stratified fluid over a flat bottom are separable into vertical and horizontal structures. The equation governing vertical structure indicates that  $w$  is linear within a mixed layer, giving another constraint on the shape of  $w(z)$ . Matching deep  $w$  behavior inferred from the non-mixing version of (3) with a linear portion in the mixed layer which vanishes at the sea surface makes possible an estimate of vertical density advection throughout the region where turbulent transport of density is important. Hence, through the assumptions stated, the PCM record of current and density profiles is sufficient to estimate the substantial derivative of density (all three terms on the left side of (3)). Vertical integration of density change following a fluid parcel then gives an estimate of turbulent mass flux  $\langle w' \rho' \rangle$ , that is, the quantity whose convergence represents mixing.

Although mixing events in the seasonal pycnocline take place on time scales identical to those of storms, even the relatively weak mesoscale eddy environment of the OCEAN STORMS site requires quantities to be smoothed temporally to yield stable estimates of

advective contributions. A filtered density record is given in Figure 7 where fluctuations with periods shorter than 20 days have been suppressed. Unfortunately, the number of weights necessary for the filter shortens the record at each end, so much so that the low-passed record begins at the onset of the October 4 storm. Contours initially within the seasonal pycnocline descend over time before eventually outcropping, indicative of mixing within the pycnocline. The second half of the record (lower frame, Figure 7) reveals little mixing activity and a tendency for the pycnocline to rise and fall due to mesoscale fluctuations. The time derivative of low-pass filtered density shows both the late fall season increase in density within the mixed layer and accompanying decrease beneath it (Figure 8). The horizontal advective contribution to density, assuming vertical shear is purely geostrophic, is comparable in size to local temporal change (Figure 9). This term (the second in equation 3) is positive within the mixed layer from late October through mid-January, indicating that lighter water is being imported laterally into the region. This tendency is nearly cancelled within the pycnocline by upwelling during this period, as evidenced by negative values of the vertical advection term  $w\rho_z$  (Figure 10). It may be noted that any error in estimating horizontal advection will necessarily tend to be cancelled by an error in the opposing sense in implied vertical advection as (3) suggests.

The vertical buoyancy flux  $-g\rho_0^{-1}\langle w'\rho' \rangle$  implied by the sum of the terms on the left side of equation (3) is given in Figure 11. While uncertainties in estimating advection make the second half of the record somewhat suspect, there is clearly a large upward buoyancy flux within the mixed layer during the fall cooling period. This flux averages roughly  $10^{-7}$  W/kg at the surface. This buoyancy flux is presumed carried by convective activity within the mixed layer. Buoyancy flux changes sign at the base of the mixed layer so that buoyancy is transported downward within the seasonal pycnocline and deposited there. This downward flux reaches values as high as  $10^{-8}$  W/kg. If turbulent mass flux is expressed as being diffusive, following the definition  $\langle w'\rho' \rangle = -K\rho_z$ , then the implied diffusivity  $K$  within the seasonal pycnocline falls in the range  $1-5 \times 10^{-4}$  m<sup>2</sup>/s. These are reasonable values for what is expected in a highly smoothed description of mixing.

## DISCUSSION AND CONCLUSIONS

The implication of the downward buoyancy flux within the seasonal pycnocline is that turbulent dissipation must be high enough to decay the observed near-inertial internal wave activity substantially. The "dissipation method" (see Gregg (1987), Osborne (1980)) declares that flux Richardson numbers in stratified turbulence are limited to values of about 0.2. Measurements in strongly sheared equatorial currents indicate the ratio of buoyancy flux to turbulent kinetic energy dissipation to be about 0.1 (Peters et al., 1988). Hence the dissipation associated with turbulence is 5 to 10 times the buoyancy flux being effected. If the buoyancy flux of turbulence in the seasonal pycnocline is  $O(10^{-8}$  W/kg), then the dissipation rate of kinetic energy must be  $O(10^{-7}$  W/kg). This is the rate at which energy is presumed removed from near-inertial motions in the OCEAN STORMS observations. A typical kinetic energy content of mixed layer near-inertial

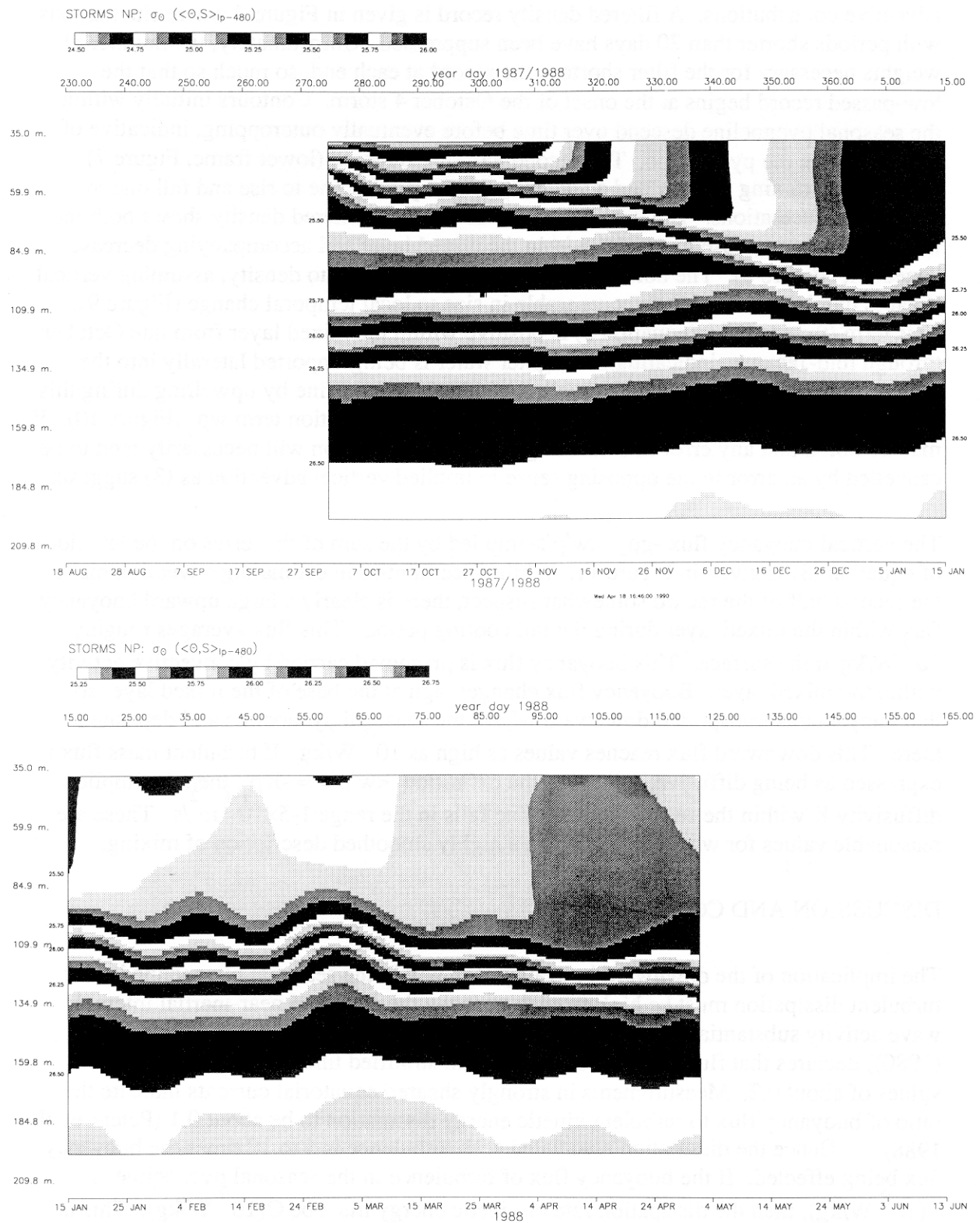


Figure 7. Low-pass filtered potential density  $\sigma_\theta$  contoured as in Fig. 1. The start and end of the record has been deleted to accommodate the filter.

# Mixing in the Seasonal Thermocline

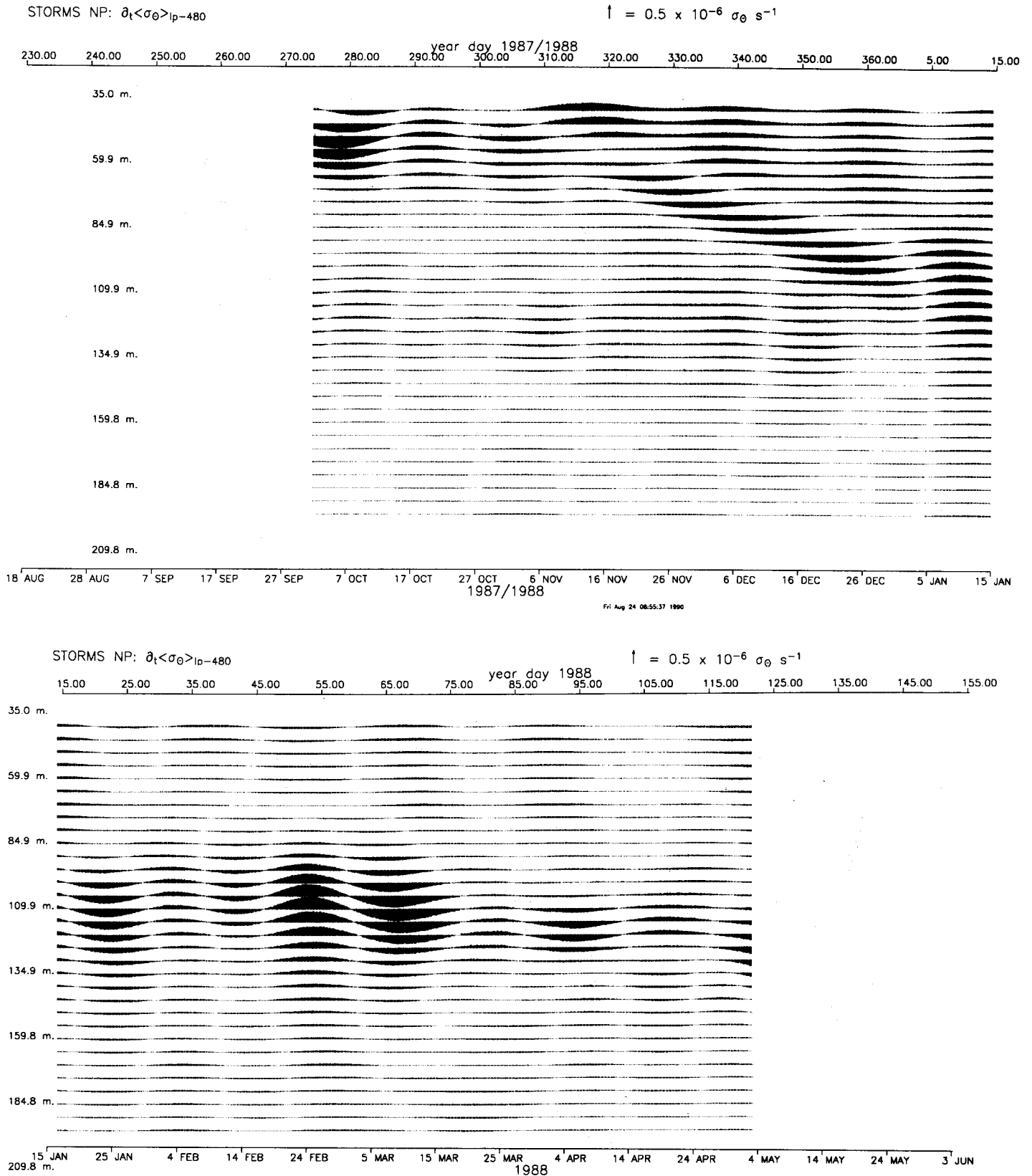


Figure 8. Time rate of change of low-pass filtered potential density where the scale in the upper right of each frame is  $0.5 \times 10^{-9} \text{ kg/m}^3/\text{s}$ .

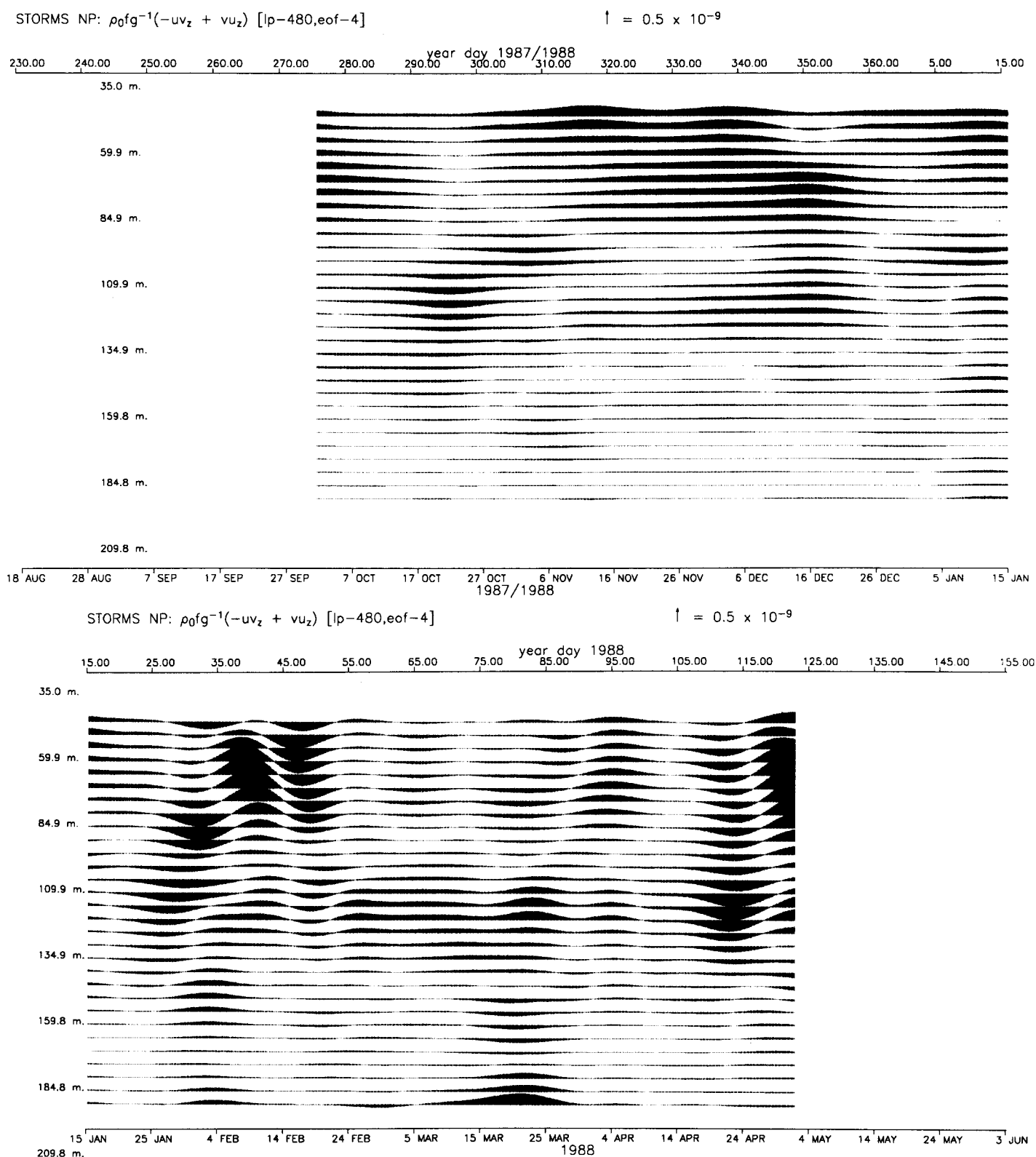


Figure 9. Horizontal advection of potential density calculated assuming vertical shear is geostrophic and plotted with the same scale as Fig. 8.



# Mixing in the Seasonal Thermocline

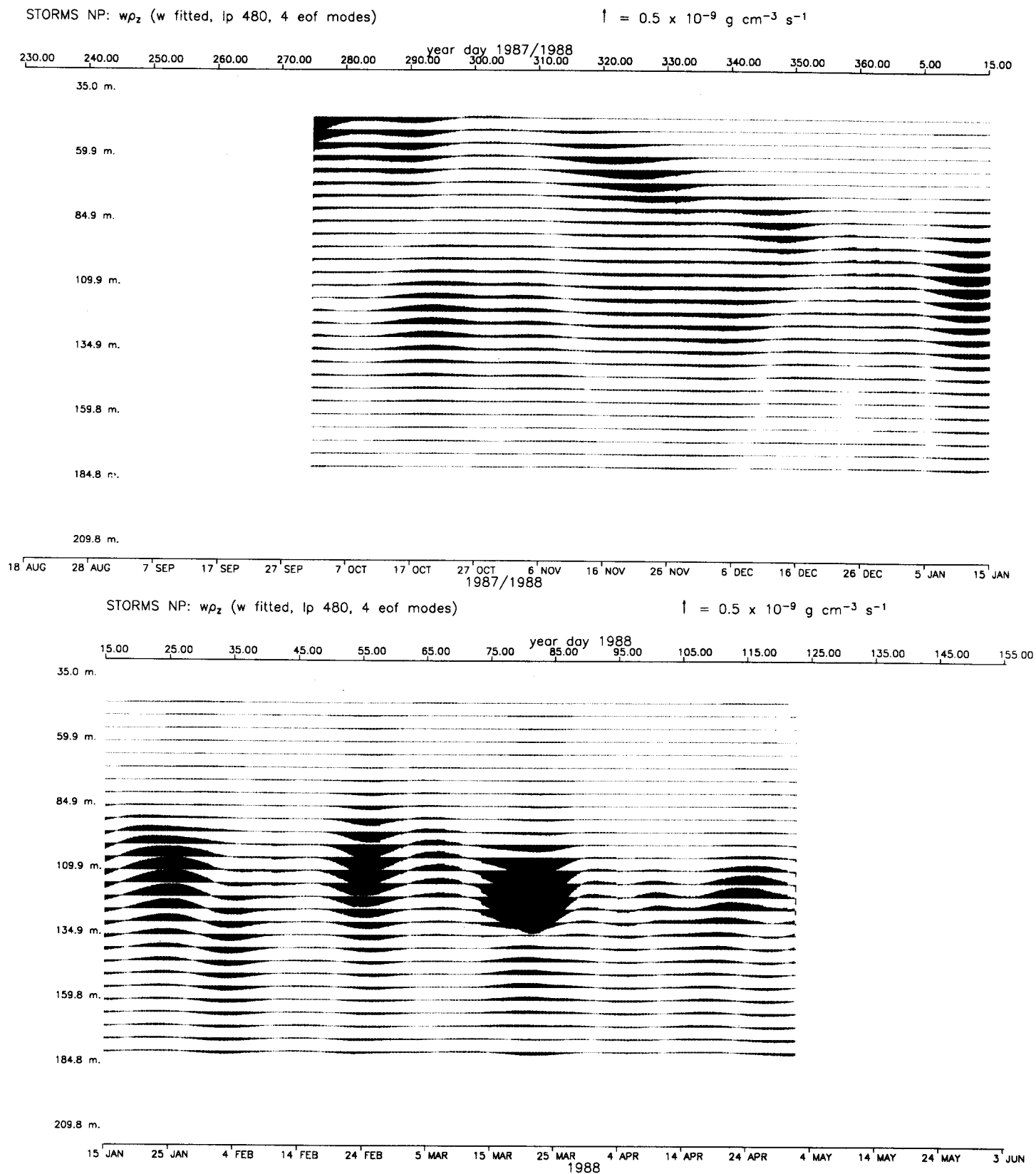


Figure 10. Vertical advection of potential density plotted as in Figs. 8 and 9.

# Eriksen

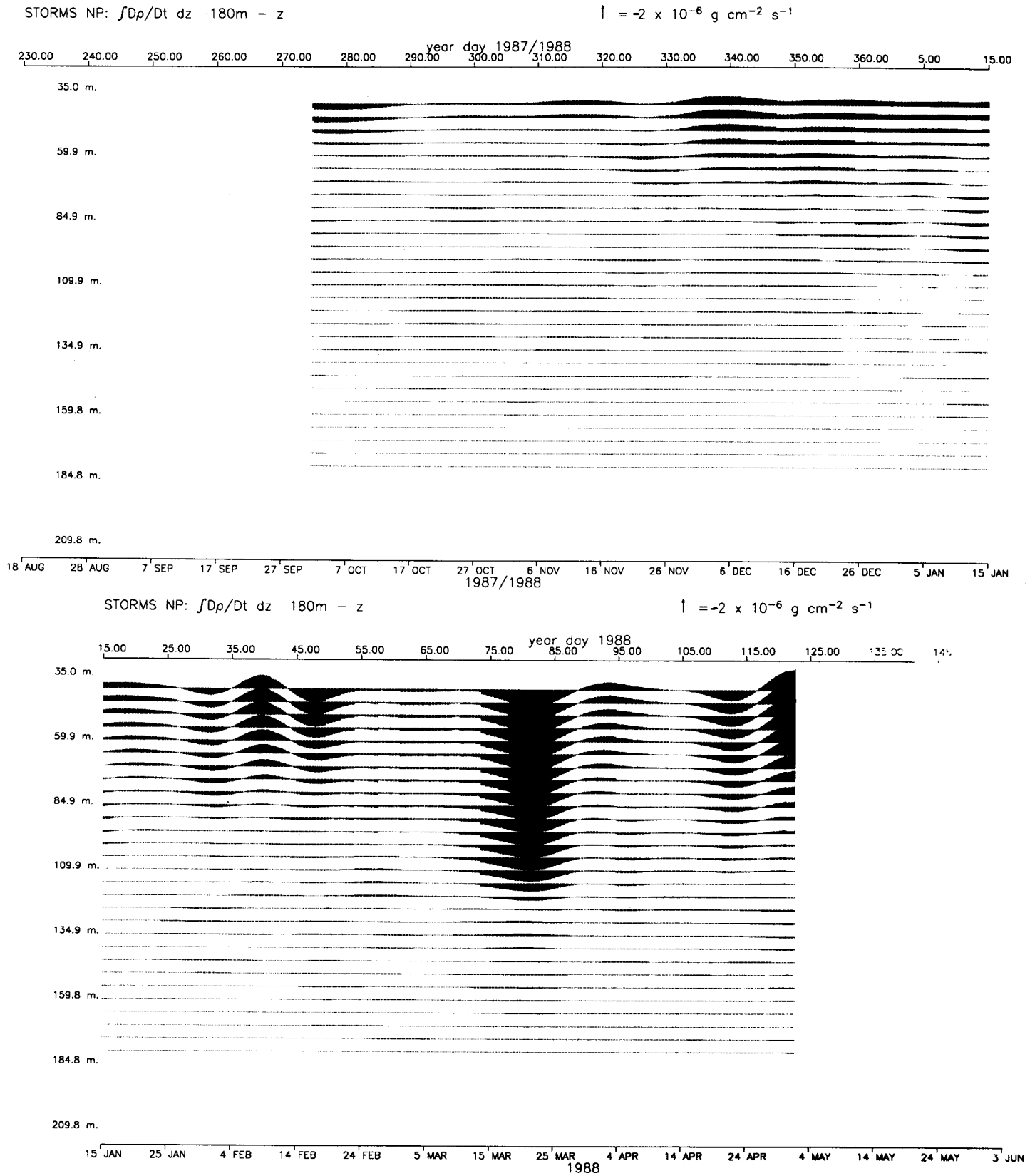


Figure 11. Vertical mass flux inferred from the vertical integral of the substantial derivative of density plotted with a scale of  $-2 \times 10^{-5} \, kg/m^2/s$  (equivalent to a buoyancy flux scale of  $2 \times 10^{-5} \, W/kg$ , i.e., an upward stick corresponds to upward buoyancy flux).

motions is the layer depth  $h$  times half the mean square current current. A decay time for mixed layer near inertial motions can then be estimated as the ratio of this to the rate of kinetic energy removal by turbulent dissipation within the pycnocline:

$$t_{\text{decay}} = hh'^{-1} \langle u^2 \rangle / \epsilon$$

where  $h'$  is the depth range over which dissipation at rate  $\epsilon$  is taking place within the pycnocline. This decay time works out to be about one week in the OCEAN STORMS observations.

The decay of near-inertial motions in the mixed layer is presumably governed by two processes: wave propagation and frictional damping. Calculations of D'Asaro (1991) demonstrate that both linear and nonlinear model simulations of the October 4 storm leave near inertial energy in the mixed layer much longer than the OCEAN STORMS observations indicate. His best simulation of the character of the descending internal wave beam include frictional damping. Our calculations of the amount of mixing that takes place as the mixed layer and seasonal pycnocline descend together imply that enough turbulent dissipation of kinetic energy must take place at the same time to extract a considerable fraction of the energy in the internal wave field. This energy is lost ultimately to dissipation at molecular scales. The picture that emerges is that a substantial portion of the near-inertial internal wave energy that would result from a given storm wind stress pattern is lost to friction through generation of shear at the base of the mixed layer in the top 20 m or so of the pycnocline. Actual wave amplitudes are reduced accordingly and a significant fraction of the work done by wind stress goes into raising potential energy of the water column through mixing by shear instability within the upper pycnocline.

## REFERENCES

- D'Asaro, E. A., 1989: The decay of wind-forced mixed layer inertial oscillations due to the  $\beta$  effect. *J. Geophys. Res.*, **94**, 2945-2056.
- D'Asaro, E. A., 1991: The need for better internal wave models. this volume
- Eriksen, C. C., J. M. Dahlen, and J. T. Shillingford, Jr., 1982: An upper ocean moored current and density profiler applied to winter conditions near Bermuda. *J. Geophys. Res.*, **87**, 7879-7902.
- Gregg, M. C., 1987: Diapycnal mixing in the thermocline: A review. *J. Geophys. Res.*, **92**, 5249-5286.
- Kundu, P. K., and R. E. Thomson, 1985: Inertial oscillations due to a moving front. *J. Phys. Oceanogr.*, **15**, 1076-1084.
- Pollard, R. T., P. B. Rhines, and R. O. R. Y. Thompson, 1973: The deepening of the wind-mixed layer. *Geophys. Fluid Dyn.*, **3**, 381-404.

- Price, J. F., R. A. Weller, and R. Pinkel, 1986: Diurnal cycling: Observations and models of the upper ocean response to diurnal heating, cooling and wind mixing. *J. Geophys. Res.*, *91*, 8411-8427.
- Osborne, T. R., 1980: Estimates of the local rate of vertical diffusion from dissipation measurements. *J. Phys. Oceanogr.*, *10*, 83-89.
- Peters, H., M. C. Gregg, and J. M. Toole, 1988: On the parameterization of equatorial turbulence. *J. Geophys. Res.*, *93*, 1199-1218.

$$\rho_t + \mathbf{u} \cdot \nabla \rho + w \rho_z = -\langle w' \rho' \rangle_z \quad (1)$$

$$\mathbf{u}_t + \mathbf{u} \cdot \nabla \mathbf{u} + w \mathbf{u}_z + 2\Omega \times \mathbf{u} + \rho_0^{-1} \nabla p = -\langle \mathbf{u}' w' \rangle_z \quad (2)$$

where the primed quantities represent turbulent microscale variations and brackets the averages of their products. The first equation states that density changes following a particle are due solely to the vertical convergence of vertical turbulent transport of density. The second states that horizontal acceleration of a fluid parcel in a rotating frame of reference is balanced by a pressure gradient force and vertical convergence of vertical turbulent transport of horizontal momentum. Turbulence is considered as any process producing non-vanishing correlation between flow components at time and space scales too small to be resolved by the observations. It is also assumed that only vertical transports of density and momentum by turbulence are important. At low frequencies the momentum balance is geostrophic provided turbulent stresses  $\tau = -\rho_0 \langle \mathbf{u}' w' \rangle$  can be ignored. This simplification is poorest within the mixed layer and is of questionable validity within the seasonal pycnocline. Nevertheless, we make it here in order to obtain estimates of horizontal density gradients through the thermal wind equations. Then (1) may be written as

$$\rho_t - f \rho_0 g^{-1} (u v_z - v u_z) + w \rho_z = -\langle w' \rho' \rangle_z \quad (3)$$

where  $f = 2\Omega \sin(\text{latitude})$  is the inertial frequency. Since we are without direct measurements of vertical velocity, we must assume that turbulent mass fluxes  $\langle w' \rho' \rangle$  effectively vanish at some depth beneath the mixed layer so that  $w$  can be estimated from (3) for the restricted depth range for which density is assumed to change purely advectively. Since  $w$  must also effectively vanish at the sea surface because changes in sea level are very slight,  $w$  can be interpolated for the mixed layer and the depth range within the pycnocline for which mixing is presumed of potential importance. The linear inviscid modes of oscillation of a rotating stratified fluid over a flat bottom are separable into vertical and horizontal structures. The equation governing vertical structure indicates that  $w$  is linear within a mixed layer, giving another constraint on the shape of  $w(z)$ . Matching deep  $w$  behavior inferred from the non-mixing version of (3) with a linear portion in the mixed layer which vanishes at the sea surface makes possible an estimate of vertical density advection throughout the region where turbulent transport of density is important. Hence, through the assumptions stated, the PCM record of current and density profiles is sufficient to estimate the substantial derivative of density (all three terms on the left side of (3)). Vertical integration of density change following a fluid parcel then gives an estimate of turbulent mass flux  $\langle w' \rho' \rangle$ , that is, the quantity whose convergence represents mixing.

Although mixing events in the seasonal pycnocline take place on time scales identical to those of storms, even the relatively weak mesoscale eddy environment of the OCEAN STORMS site requires quantities to be smoothed temporally to yield stable estimates of